Complex Active Optical Networks as a New Laser Concept

Stefano Lepri,[1] Cosimo Trono,[2] and Giovanni Giacomelli[1]
[1]*Consiglio Nazionale delle Ricerche, Istituto dei Sistemi Complessi, Via Madonna del Piano 10 I-50019 Sesto Fiorentino, Italy*
[2]*Consiglio Nazionale delle Ricerche, Istituto di Fisica Applicata Nello Carrara, Via Madonna del Piano 10 I-50019 Sesto Fiorentino, Italy*
(Received 1 December 2016; published 21 March 2017)

Complex optical networks containing one or more gain sections are investigated, and the evidence of lasing action is reported; the emission spectrum reflects the topological disorder induced by the connections. A theoretical description compares well with the measurements, mapping the networks to directed graphs and showing the analogies with the problem of quantum chaos on graphs. We show that the interplay of chaotic diffusion and amplification leads to an emission statistic with characteristic heavy tails: for different topologies, an unprecedented experimental demonstration of Lévy statistics expected for random lasers is here provided for a continuous-wave pumped system. This result is also supported by a Monte Carlo simulation based on the ray random walk on the graph.

DOI: 10.1103/PhysRevLett.118.123901

Pursuing laboratory investigations of complex dynamics on networks is a topic of growing interest motivated, e.g., by the study of power grids and their failures [1], the role of topology on synchronization [2], or other nonlinear effects [3,4]. In this Letter, we present a novel scheme: the *lasing network* (LANER). It consists of a complex active optical network, whose connectivity induces a form of topological disorder and can display laser action. Besides its intrinsic interest, the system may be regarded as an optical implementation of a dynamical system on a graph [5]. The great majority of lasers share the same structure with a single gain section in a simple linear or ring cavity, supporting regular sets of optical modes [6]. A somehow opposite case is the random laser, where the propagation of rays in a disordered gain medium leads to light amplification [7,8]. The LANER generalizes to strongly connected multiple gain setups and could also be considered as a *discrete* random laser with a controllable complexity. The robustness and flexibility of the apparatus permit us to explore different configurations by an easy rearrangement of the components; the stability of the setup allows for detailed statistical analysis as well.

The network we consider is built with N_s couplers connected by N_l single-mode fibers, some of them (*active*) capable to provide optical amplification via stimulated emission. The couplers are standard optical power splitters or other commercially available components such as circulators, etc. Isolators can also be used to select a propagation direction; in the present Letter, we will deal only with directed active fibers and 2×2 (four ports) lossless couplers with no open ports so that $N_l = 2N_s$. Schemes of the simplest topologies with $N_s = 1$ and 2 realized experimentally are depicted in Fig. 1 (curves with white background). Alongside, their representation as equivalent *directed graphs* is given (see below).

For the theoretical description, we denote by L_j the lengths of the N_l fiber segments and by g_j the respective gain ($g_j > 1$) or loss ($g_j < 1$) factors. The observables are the envelopes of the longitudinal optical field propagating in opposite directions along each fiber. Within a linear description, where nonlinear dispersion, gain saturation, etc. are disregarded, the optical spectrum is determined through the $2N_l \times 2N_l$ network matrix $N = PS$ in terms of the *propagation* matrix P (which contains the metric and topological information) and the wave splitting at the couplers through the unitary *scattering* matrix S (see Supplemental Material [9]). Assuming that the field through the link j is multiplied by a factor $G_j = g_j e^{iKL_j}$, the allowed complex wave numbers K (poles) are determined by the condition $\det[N(K) - I] = 1$, where I is the $2N_l \times 2N_l$ identity matrix. This generalizes the usual mode-matching and threshold conditions for a laser in the case of linear gains and no cross phase-gain coupling. Its analytic solution is usually unfeasible even for the simplest networks, but it can be solved numerically.

A representation of the LANER in terms of graphs can be introduced as well by setting all the nonzero elements of the matrix N to 1 and defining the result as the adjacency matrix of the equivalent graph. In such a picture, each vertex represents a component of the field in a link; a directed bond indicates the linear dependence of the target on the source mode. An empty (red) vertex indicates that the related mode link is active, otherwise passive if filled (see Fig. 1). The inclusion of isolators in the active links leads to the removal of the blocked fields, and therefore, the corresponding vertices are removed from the equivalent graph, which is *pruned*. It is worth noting that the system can lase only if at least one active vertex is present in the pruned graph. At the simplest level of description, the

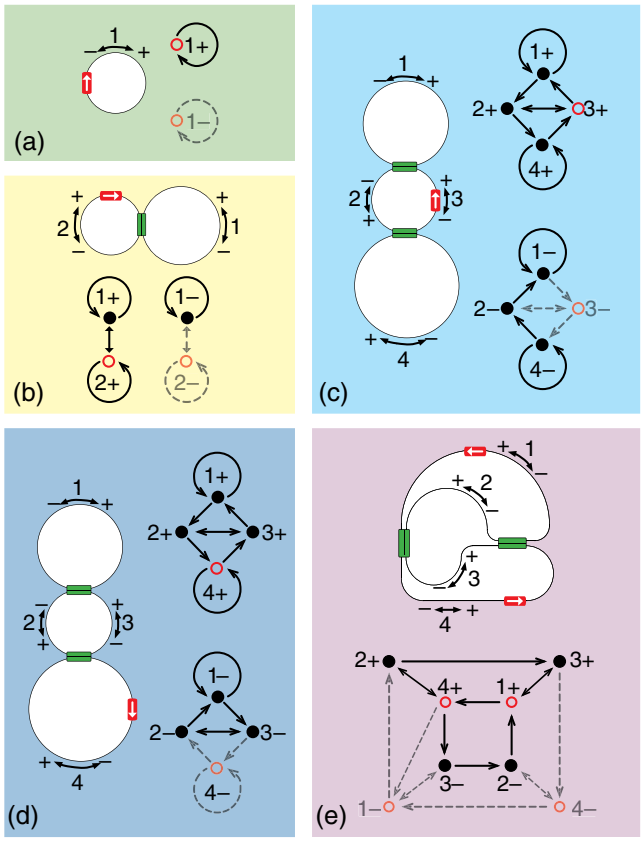

FIG. 1. Simpler LANERs (white) and their equivalent graphs. Arrowed (red) segments represent oriented gain sections, numbered (black) arrows the modes in the links. Graphs: (red) circumferences denote active links modes.

photon dynamics in the LANER can be visualized as a Markovian random walk [10] on such graphs.

We remark the close analogies of this scheme with the *quantum graphs*, which have been thoroughly investigated in the realm of quantum chaos [11,12]. Indeed, in the Hamiltonian case ($g_j = 1$), N (termed the vertex scattering matrix) is unitary. The equation for the poles is formally equal to the one to determine the quantum spectrum of a particle moving freely along the bonds and scattered at the graph vertices. In this context, open graphs have been also considered [13,14]. Experimentally, quantum graphs can be simulated by microwave networks [15]. Besides the different physical nature of our system, an important novel and controllable element that we deal with here is the optical gain (possibly in multiple links), which allows us to achieve the lasing action and investigate entirely new effects.

We start our investigation in the setup corresponding to the network or graph of Fig. 1(c) (Fig. 1 of the Supplemental Material [9]). The first feature that we demonstrate is the existence of a well-defined threshold for lasing, which manifests experimentally as a sudden switching of an increasingly large number of distinct peaks in the emission spectrum upon the increasing of the pump current. Figure 2(a) shows the onset of the laser action in the experiment, while Figs. 2(b)–2(c) report the related results from the theory. In the experiment, at low pump values, the spectrum is flat, and no emission is visible at any frequency; then, some peaks appear and, further increasing the pump, the peaks' structure becomes more and more complicated. Their interaction between such an increasing number of active modes is not apparently strong enough to determine a standard chaotic dynamic. Figure 2(b) reports the histogram of the beatings obtained from the computation of the poles $K_n = k_n - i\mu_n$: all of the possible differences in frequency are evaluated for the lasing modes (those with $\mu_n > 0$), and their distribution is plotted. The result gives a qualitative estimation of the beating spectrum and directly compares to the experiment, showing the same complex hierarchical structure. The poles K_n for the same geometry are reported in the complex plane for increasing gain in the active fiber [Fig. 2(c)]. Above a critical value, a set of resonances cross the real axis, and the associated modes grow with rate $\mu_n > 0$ and start to lase. Since we assumed an infinite gain bandwidth, the dynamics above threshold will be very high dimensional [12]. In the experiment, the number of active modes will be limited by the gain bandwidth. For the case at hand (Er^{3+}-doped medium), this is estimated to be of the order of some tens of nm so that more than 10^5 modes may be excited. The peaks' frequency is not significantly affected by the pumping, indicating that the nonlinearity only saturates the amplitude, and gain dispersion is negligible.

The above results are reminiscent of highly multimode lasers' behavior; however, the possible choice of complex network topologies and arbitrary numbers of gain sections permit a generalization of the geometries for, e.g., longitudinal lasers. Moreover, this sets the peculiar statistical features of our system that we discuss below.

The classical dynamics of particles on graphs is a chaotic type of diffusive process [16] that can be described theoretically by simple one-dimensional piecewise chaotic maps [17]. It is well known that this reflects in the statistical properties of the spectra as thoroughly investigated in the quantum chaos literature. For comparison, we numerically computed the nearest-neighbor level spacing distribution $P(s)$, where $s = (k_{n+1} - k_n)/\bar{s}$ are normalized to the average $\bar{s}$. All the computed k_n were included in the analysis regardless of the sign of μ_n and the distributions averaged over a set of graphs with the same topology and random lengths. Even for the case above threshold, Fig. 2(d) shows that $P(s)$ resembles the Wigner-Dyson distribution $\pi s \exp(-\pi s^2/4)/2$ typical of chaotic systems [12]. Actually, individual realizations typically display a level repulsion similar to that demonstrated for the Hamiltonian case [18], but deviations are expected in view of the smallness of the graph.

In Fig. 2(e), we also report the Fourier transform of the beating spectrum $F(l)$, which is closely related to the

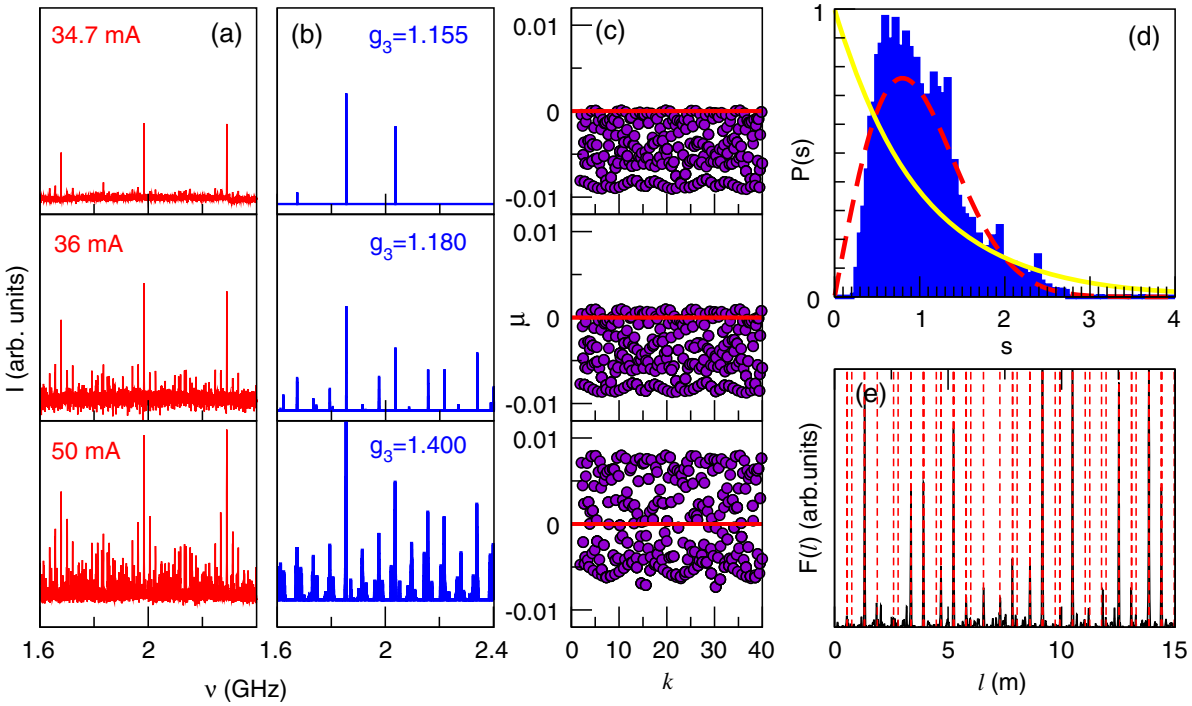

FIG. 2. Results for the LANER in Fig. 1(c), with $L_1 = 9.16$ m, $L_2 = 18.12$ m, $L_3 = 5.24$ m, $L_4 = 10.0$ m. (a) Experimental intensity spectrum increasing the pump current. Numerics: (b) beatings for increasing g_3 at fixed $g_1 = g_2 = g_4 = 0.9$, (c) poles in the complex plane, (d) level spacing distribution, averaged over an ensemble of 30 graphs (10^4 poles each) with the same topology, $g_1 = g_2 = g_4 = 0.9$, $g_3 = 1.4$ and uniformly distributed random L_j with average 10. Wigner (dashed) and Poisson (solid) distributions are plotted for comparison. (e) Experimental length spectrum [see Eq. (4) in the Supplemental Material [9]] at $J = 80$ mA; the vertical lines represent the combinations $mL_1 + n(L_2 + L_3) + lL_4$ with m, l, n integers.

length spectrum (see Supplemental Material [9]); it is experimentally accessible and relates the spectra to the underlying classical periodic orbits [12,15]. In particular, the experimental results (black peaks) well fit the theoretical prediction (vertical red lines), expressing the lengths as a combination of the three *ring* paths of lengths L_1, $L_2 + L_3$, and L_4: L_2 and L_3 are not contributing independently as expected.

The interplay of diffusion and amplification of photons in scattering media, as it occurs in random lasers [7,8], can lead to heavy-tailed distributions of emission intensities, characterized by Lévy-stable statistics [19]. This theoretical prediction [20] (see also [21,22]) has been confirmed in several experiments [23–25]. To the extent in which the photons in our networks can be treated as particles undergoing chaotic diffusion, it is thus plausible that the same phenomenology may also occur in the LANER. We consider first the configuration in Fig. 1(b). As evidenced by the graph, it may represent the simpler scheme in our setup where orbits with gain and with losses coexist, thus realizing the basic scenario for chaotic diffusion with gain. This is indeed the case, as shown in Fig. 3. Using a time-resolved analysis of the amplitude behavior of the peaks, the dynamics of the emission intensity at $\nu = 163.57$ MHz is reported in Figs. 3(a) and 3(b). The emission shows rare large spikes with strong intermittent fluctuations both in amplitude and time duration. In Fig. 3(c), we present the histograms $P(I)$ of such emission, exhibiting a clear evidence of a Lévy process (magenta dashed line). For the same pump current, other peaks display instead a log-normal distribution; e.g., we show in the figure the case of $\nu = 191.94$ MHz (yellow). The same results can be found in the configuration in Fig. 1(c) [a distribution is shown in the inset of Fig. 3(c)] in spite of the different location of the gain [now in the link (4)] in the configuration in Fig. 1(d).

The fact that anomalous fluctuations only occur at some beating frequencies can be justified as follows. In analogy with the random laser case [20], we expect fluctuations to occur only for modes which are close enough to threshold, namely those with $|\mu_n| < \varepsilon$, with ε being some small characteristic value. If, as suggested by Fig. 2(c), the poles' density is roughly uniform, the typical spectral separation between such modes is inversely proportional to ε. Thus, strongly fluctuating modes will only contribute to the subset of the beatings lying at a distance of order $1/\varepsilon$, while only far-from-threshold modes will contribute to the remaining, yielding log-normal statistics.

To further check the interpretation, we consider the two cases of Fig. 1(a) and Fig. 1(e). In the former, only orbits with gain are possible, thus indicating the settling of saturated log-normally distributed peaks at the cavity resonances. This is indeed expected as the configuration

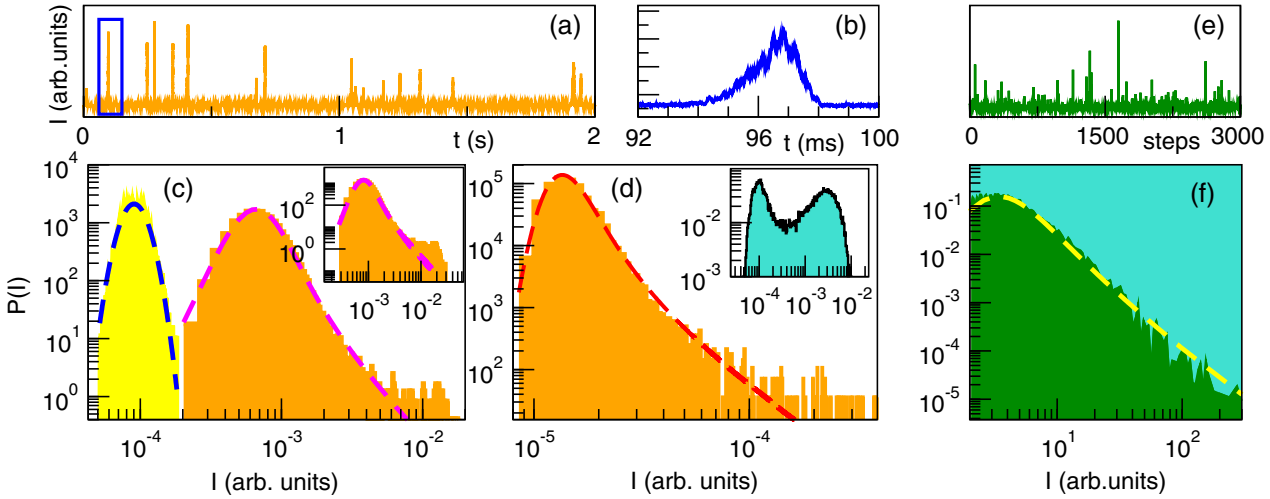

FIG. 3. LANER emission dynamics and statistics. (a)–(d): Experiment. Setup of Fig. 1(b). (a) Time-resolved intensity at $\nu = 163.57$ MHz. (b) Boxed event in (a). (c) Distributions of intensity for $J = 42.2$ mA: left, $\nu = 191.94$ MHz, (blue) dashed line, log-normal fit; right, $\nu = 163.57$ MHz, (magenta) dashed line, Lévy stable fit with $\alpha = 1.4$; inset, setup of Fig. 1(c), distribution at $\nu = 327.13$ MHz for $J = 37.0$ mA, (magenta) dashed line, Lévy stable fit with $\alpha = 1.4$. (d) Setup of Fig. 1(e): distribution of the intensity of the mode **3+** at $\nu = 380.25$ MHz for $J_1 = 10$ mA (link with losses) and $J_4 = 55$ mA (link with gain); (red) dashed line, Lévy stable fit with $\alpha = 1.32$; inset, bistable distribution at $\nu = 380.34$ MHz for $J_1 = 40$ mA and $J_4 = 60$ mA (both links have gain). Monte Carlo simulation, geometry of Fig. 1(c) (see Supplemental Material [9]). (e) Time series. (f) Distribution of (e), (yellow) dashed line, Lévy stable fit with $\alpha = 0.995$.

realizes the standard monodirectional ring laser: without the isolator, the network would be represented by two *disjoint* active graphs, with bistable statistics describing the random jumps between the two emitted modes.

In the latter, a more complicated situation appears due to the effect of two gains. We first consider that the link (1) only in Fig. 1(e) provides gain [the link (4) is now passive; i.e., its laser pump current is kept sufficiently low]. Here, we found the same phenomenology reported above; an example of the Lévy statistics for a peak is reported in Fig. 3(d). As a second case, we increase the pump current in link (4) so that it has gain as well. The distribution now shows a multistable shape (see inset); an inspection of the equivalent graph reveals that there aren't orbits without gain. Thus, besides the complex geometry of the network, we are dealing with an extension of the ring laser: the multistability arises from the system switching between the saturated modes of the cavity.

To strengthen the theoretical description, we have compared the experimental findings with a Monte Carlo type of model (see Supplemental Material [9]). The simulation scheme propagates a set of rays through the network, assigning an intensity, each that grows or decreases depending on the local value of the gains g_j. Whenever a ray reaches a splitter, it is transmitted towards one of the connected fibers chosen at random: the transition probability is given by the splitting factors. Altogether, the ray motion is a random walk on the graph, while the accumulated intensity depends on the whole walk history. The simulation data [for the case of Fig. 1(c)] are presented in Fig. 3(e), showing the temporal behavior of the intensity collected at one point of the network. The distribution of the data is well fitted with a Lévy distribution [Fig. 3(f)].

To conclude, we have presented the LANER as an optical scheme showing laser action and characterized by a fully controllable topological disorder. We studied its emission statistics at the laser threshold, evidencing heavy-tails fluctuations with Lévy distribution. They are the typical signature of the interplay of chaotic diffusion and amplification of the photons in the network and indicate that the LANER represents an intermediate case between the standard and the random laser. In particular, the possibility to include multiple and independent gain sections is shared with the latter, but the scheme we have introduced has several advantages in terms of flexibility and control. For instance, it is continuous-wave pumped at variance with standard random laser experiments. From the point of view of basic research, the LANER would allow different investigations, ranging from dynamics on networks of increasing complexity to the effect of the cavity topology on the laser emission.

We thank F. Cherubini, G. P. Puccioni, and acknowledge a partial support from EU Project No. 289146 (NETT).

[1] M. Rohden, A. Sorge, M. Timme, and D. Witthaut, Phys. Rev. Lett. **109**, 064101 (2012).
[2] I. Belykh, M. Hasler, M. Lauret, and H. Nijmeijer, Int. J. Bifurcation Chaos Appl. Sci. Eng. **15**, 3423 (2005).
[3] S. Gnutzmann, U. Smilansky, and S. Derevyanko, Phys. Rev. A **83**, 033831 (2011).

[4] F. Perakis, M. Mattheakis, and G. Tsironis, J. Opt. **16**, 102003 (2014).
[5] M. A. Porter and J. P. Gleeson, *Dynamical Systems on Networks: A Tutorial* (Springer, New York, 2016).
[6] P. W. Milonni and J. H. Eberly, *Laser Physics* (John Wiley & Sons, Hoboken, NJ, 2010).
[7] H. Cao, Waves Random Media **13**, R1 (2003).
[8] D. S. Wiersma, Nat. Phys. **4**, 359 (2008).
[9] See Supplemental Material at http://link.aps.org/supplemental/10.1103/PhysRevLett.118.123901 for details.
[10] R. Burioni and D. Cassi, J. Phys. A **38**, R45 (2005).
[11] P. Kuchment, Waves Random Media **14**, S107 (2004).
[12] T. Kottos and U. Smilansky, Ann. Phys. (N.Y.) **274**, 76 (1999).
[13] F. Barra and P. Gaspard, Phys. Rev. E **65**, 016205 (2001).
[14] T. Kottos and U. Smilansky, J. Phys. A **36**, 3501 (2003).
[15] O. Hul, S. Bauch, P. Pakoński, N. Savytskyy, K. Życzkowski, and L. Sirko, Phys. Rev. E **69**, 056205 (2004).
[16] F. Barra and P. Gaspard, Phys. Rev. E **63**, 066215 (2001).
[17] P. Pakonski, K. Zyczkowski, and M. Kus, J. Phys. A **34**, 9303 (2001).
[18] F. Barra and P. Gaspard, J. Stat. Phys. **101**, 283 (2000).
[19] V. V. Uchaikin and V. M. Zolotarev, *Chance and Stability: Stable Distributions and Their Applications* (Walter de Gruyter, Utrecht, The Netherlands, 1999).
[20] S. Lepri, S. Cavalieri, G. L. Oppo, and D. S. Wiersma, Phys. Rev. A **75**, 063820 (2007).
[21] S. Lepri, Phys. Rev. Lett. **110**, 230603 (2013).
[22] E. P. Raposo and A. S. L. Gomes, Phys. Rev. A **91**, 043827 (2015).
[23] E. Ignesti, F. Tommasi, L. Fini, S. Lepri, V. Radhalakshmi, D. Wiersma, and S. Cavalieri, Phys. Rev. A **88**, 033820 (2013).
[24] R. Uppu and S. Mujumdar, Phys. Rev. A **90**, 025801 (2014).
[25] A. S. Gomes, E. P. Raposo, A. L. Moura, S. I. Fewo, P. I. Pincheira, V. Jerez, L. J. Maia, and C. B. De Araújo, Sci. Rep. **6**, 27987 (2016).